FSU-HEP-040110

EPJdirect (2008), to be processed by the editorial

EPJdirect
electronic only

Production of Excited Neutrino at LHC

A. Belyaev[1], C. Leroy[2], R. Mehdiyev[2,3]

[1] Department of Physics, Florida State University, Tallahassee, FL, USA.
[2] Université de Montréal, Département de Physique, Montréal, H3C 3J7, Canada.
[3] on leave of absence from Institute of Physics, Azerbaijan National Academy of Sciences, 370143, Baku, Azerbaijan.

Abstract. We study the potential of the CERN LHC in the search for the single production of excited neutrino through gauge interactions. Subsequent decays of excited neutrino via gauge interactions are examined. The mass range accessible with the ATLAS detector is obtained.

PACS: 12.60.Rc, 13.85.Rm

1 Introduction

The proliferation of quarks and leptons can be naturally explained by the assumption that they are composite objects. According to models of compositeness[1], known fermions are bound states of more fundamental constituents – preons [2] or a fermion and a boson [3]. In the framework of these models, constituents of known fermions interact by means of new strong gauge interactions.

One of the main consequences of the non-trivial substructure of the standard model (SM) fermions would be a rich spectrum of excited states[1, 4]. Observation of such fermionic excitations would be clear evidence of the underlying subtructure of known fermions. Therefore, one of the tasks of great importance for TeV energy scale colliders is to probe possible substructures of leptons and quarks and test the variety of compositeness models.

The SM can be considered as the low energy limit of a more fundamental theory which is characterized by a large mass scale Λ. The existence of four-fermion contact interactions would be a signal of new physics beyond the SM. The nature of this new physics can be probed if the experimental energy scale is high enough. It is expected that the next generation of hadron colliders like the LHC, which will achieve very high centre of mass energies, will extend the search for composite states. In particular, contact interactions may be an important source for excited lepton production at the CERN LHC.

The excited states of the SM fermions can interact via SM gauge field interactions and also via new gauge strong interactions between preons. The later leads to effective contact interactions between quarks and leptons and/or their excited states in the low energy limit.

Many recent experimental studies have been devoted to the search for quark and lepton compositeness and excited states at LEP([5]), HERA([6]), and TEVATRON([7]). No signals from contact interactions and excited fermions have been found so far. Studies mentioned above put limits: i) on the compositeness scale in the range of 2-8 TeV, depending on the type of the contact interactions, and ii) on the excited fermion mass up to the collider center-of-mass energy.

Based on previous studies [8, 4, 9, 10, 11], we expect that the LHC collider will put the most stringent constraints on the composite models and/or the masses of excited fermions.

This paper aims at a study of the potential of LHC collider in the search for the excited neutrino production which has not been studied in details, previously. This work is a continuation of previous works devoted to the study of the excited quark and excited electron production [9].

The paper is organized as follows. In Section 2 we discuss effective Lagrangians for models used for our study. Section 3 presents details of our study and results, while Section 4 outlines the conclusions.

2 Physical setup

For the sake of simplicity we limit the number of parameters in our study and assume the most simple realization of a model where the spin of the excited fermions is $\frac{1}{2}$ and that they are isospin $\frac{1}{2}$ partners (higher spin representations are considered in [12], for example).

We assume also that an excited fermion has acquired mass before SU(2)⊗U(1) symmetry breaking. Therefore, we consider their left- and their right- components in isodoublets. For example, we have the following assignments for the first generation of fermions:

$$l_L = \begin{pmatrix} \nu_e \\ \mathrm{e} \end{pmatrix}_L \ , \ e_R \qquad ; \ \ l_L^* = \begin{pmatrix} \nu_e^* \\ \mathrm{e}^* \end{pmatrix}_L \ , \ l_R^* = \begin{pmatrix} \nu_e^* \\ \mathrm{e}^* \end{pmatrix}_R$$

$$q_L = \begin{pmatrix} \mathrm{u} \\ \mathrm{d} \end{pmatrix}_L , q_R = \begin{pmatrix} \mathrm{u} \\ \mathrm{d} \end{pmatrix}_R \ ; \ \ q_L^* = \begin{pmatrix} \mathrm{u}^* \\ \mathrm{d}^* \end{pmatrix}_L \ , \ q_R^* = \begin{pmatrix} \mathrm{u}^* \\ \mathrm{d}^* \end{pmatrix}_R .$$

Let us note that in order to avoid conflict with precision measurements of anomalous magnetic moment of muon (g-2) and protect light fermions from large radiative corrections one should require a chiral form of interactions of excited fermions with SM ones [13].

The couplings of excited fermions ($f^* = l^*, q^*$) to gauge bosons are vector like:

$$L_{\mathrm{eff}}^{1gauge} = \bar{f^*}\gamma^\mu (f_s g_s \frac{\boldsymbol{l^a}}{2}\boldsymbol{G^a}_\mu + g\frac{\boldsymbol{\tau}}{2}\boldsymbol{W}_\mu + g^{'}\frac{Y}{2}B_\mu) f^*, \tag{1}$$

while transitions between ordinary and excited fermions are uniquely fixed by magnetic-moment type gauge-invariant interactions [14]:

$$L_{\mathrm{eff}}^{2gauge} = \frac{1}{2\Lambda}\bar{f}_{\mathrm{R}}^* \sigma^{\mu\nu}(f_s g_s \frac{\boldsymbol{\lambda^a}}{2}\boldsymbol{G^a}_{\mu\nu} + fg\frac{\boldsymbol{\tau}}{2}\boldsymbol{W}_{\mu\nu} + f^{'}g^{'}\frac{Y}{2}B_{\mu\nu}) f_{\mathrm{L}} + \mathrm{h.c.}, \tag{2}$$

where Λ is the compositeness scale. $\boldsymbol{G^a}_{\mu\nu}$, $\boldsymbol{W}_{\mu\nu}$ and $B_{\mu\nu}$ are SU(3), SU(2) and U(1) tensors with the coupling constants g_s, g and $g^{'}$, respectively; Y is the weak hypercharge with Y = (-1) and (1/3) for leptons and quarks, respectively; f_s, f and f' are parameters depending on the underlying dynamics.

Lagrangian 2 gives rise to the following $fermion - fermion^* - gauge\ boson$ vertices:

$$\Gamma_\mu^{g\bar{f^*}f} = \frac{g_s f_g}{2\Lambda} q^\nu \sigma_{mu\nu}(1-\gamma^5) \tag{3}$$

$$\Gamma_\mu^{\gamma\bar{f^*}f} = \frac{e}{2\Lambda}[e_f f' + T_3(f-f')] q^\nu \sigma_{mu\nu}(1-\gamma^5) \tag{4}$$

$$\Gamma_\mu^{Z\bar{f^*}f} = \frac{e}{2\Lambda}\frac{I_3(c_w^2 f + s_w^2 f') - 4e_f s_w^2 f'}{s_w c_w} q^\nu \sigma_{mu\nu}(1-\gamma^5) \tag{5}$$

$$\Gamma_\mu^{W\bar{f^*}f} = \frac{e}{2\Lambda}\frac{f}{\sqrt{2}s_w} q^\nu \sigma_{mu\nu}(1-\gamma^5) \tag{6}$$

Fig. 1. Diagrams for single excited neutrino ($\nu^\star$) production via photon and Z-boson exchange.

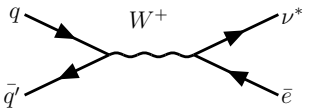

Fig. 2. Diagram for single excited neutrino ($\nu^\star$) production via W-boson exchange.

Excited fermions can be produced in pairs via interactions given by Eq. (1) as well as produced singly via interactions given by Eq. (2). In this paper, we study single excited neutrino production as the most promising reaction, since it is less kinematically suppressed compared to the case of production of the pair of excited neutrinos. Excited neutrino can be singly produced at the LHC according the process:

$$q\bar{q} \to \nu\nu^\star \tag{7}$$

i.e. via neutral current (see Fig. 1) and via the charged current, in association with an electron (see Fig. 2)

$$q\bar{q'} \to e\nu^\star. \tag{8}$$

The couplings f and f' involved in the single excited neutrino production are not equal to each other, in general. Therefore, the $\gamma\nu\nu^*$ coupling which is proportional to $(f - f')$ can be non-vanishing. In Fig. 3, we present cross sections for the processes (7) and (8) as a function of the excited neutrino mass, $m^\star$ ($\Lambda = m^\star$) for two cases: $f = f' = 1$ and $f = -f' = 1$. The respective values for the cross sections are presented in Table 1. The cross section values were calculated using the CTEQ5L parton distribution function (PDF)[20]. The QCD scale has been chosen equal to the excited neutrino mass. We have checked that the systematical uncertainty due to the choice of others PDF sets is about 20%.

Excited neutrinos will decay to $\nu\gamma$, νZ and eW products, therefore, giving rise to $\nu\nu\gamma$, $\nu\nu\nu$, νll, νqq, $e\nu l$ and eqq particles in the final state. Branching ratios for excited neutrino decay which are defined by gauge interactions and f and f' couplings are presented in Table 2. One can see that for non-vanishing $\gamma\nu\nu^*$ couplings $f = -f' = 1$, the branching ratio, $Br(\nu^* \to \gamma\nu)$, is of the

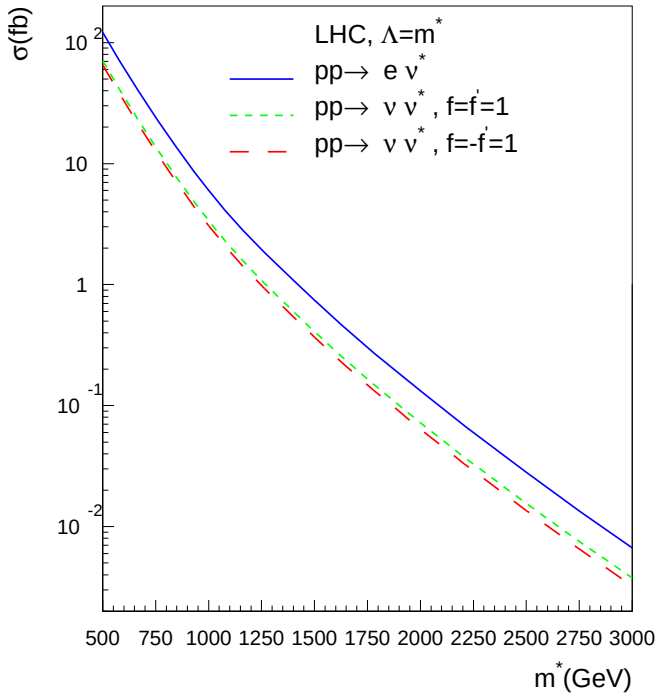

Fig. 3. Cross section of the single excited neutrino production versus the excited neutrino mass, $m^\star$ at LHC for $\Lambda = m^\star$. Dashed and dotted line denote $f = f' = 1$ and $f = -f' = 1$ choices, respectively, for the case of excited neutrino production via neutral currents. The cross sections shown account for the production of b oth excited neutrino and excited anti-neutrino at LHC.

order of 30%, therefore the role of the $\nu\gamma$ channel would be significant in this case. For the excited neutrino masses $m^\star > 500$ GeV$>> M_Z, M_W$, the branching ratio of the excited neutrino decay does not depend on their masses (see Table 2).

Table 1. Cross sections (CompHEP) (in fb) for $q\overline{q} \rightarrow \nu^\star l$ and scale $\Lambda = m^\star$

$m^\star$(GeV)		500	1000	1500	2000	2500
pp $\rightarrow e\nu^\star$		121.	5.99	7.43×10^{-1}	1.32×10^{-1}	2.82×10^{-2}
pp $\rightarrow \nu\nu^\star$	$f = f' = 1$	65.3	3.07	3.67×10^{-1}	6.40×10^{-2}	1.36×10^{-2}
	$f = -f' = 1$	70.5	3.37	4.09×10^{-1}	7.21×10^{-2}	1.55×10^{-2}

Table 2. Branching ratios(in %) of excited neutrino decay via gauge interactions for $\Lambda = m^\star$

process		for $m^\star$(GeV)	
		500	> 1000
$f = f' = 1$	$\nu^* \rightarrow We$	61	61
	$\nu^* \rightarrow Z\nu$	39	39
	$\nu^* \rightarrow \gamma\nu$	0	0
$f = -f' = 1$	$\nu^* \rightarrow We$	60	61
	$\nu^* \rightarrow Z\nu$	12	12
	$\nu^* \rightarrow \gamma\nu$	28	27

3 Simulations and results

The simulations of excited lepton signal and relevant backgrounds were performed with COMPHEP[24], the COMPHEP-PYTHIA interface[25] and PYTHIA[23] programs chain. The ATLFAST[26] code has been used to take into account the experimental conditions prevailing at LHC for the ATLAS detector. The detector concept and its physics potential have been presented in the ATLAS Technical Proposal[27] and the ATLAS Technical Design Report[28]. The ATLFAST program for fast detector simulations accounts for most of the detector features: jet reconstruction in the calorimeters, momentum/energy smearing for leptons and photons, magnetic field effects and missing transverse energy. It provides a list of reconstructed jets, isolated leptons and photons. In most cases, the detector dependent parameters were tuned to values expected for the performance of the ATLAS detector obtained from full simulation.

The electromagnetic calorimeters were used to reconstruct the energy of leptons in cells of dimensions $\Delta\eta \times \Delta\phi = 0.025 \times 0.025$ within the pseudorapidity range $-2.5 < \eta < 2.5$; ϕ is the azimuthal angle. The electromagnetic energy resolution is given by $0.1/\sqrt{E}(GeV) \bigoplus 0.007$ over this pseudorapidity (η) region. The electromagnetic showers are identified as leptons when they lie within a cone of radius $\Delta R = \sqrt{(\Delta\eta)^2 \times (\Delta\phi)^2} = 0.2$ and possess a transverse energy $E_T > 5$ GeV. Lepton isolation criteria were applied, requiring a distance $\Delta R > 0.4$ from other clusters and maximum transverse energy deposition, $E_T < 10$ GeV, in cells in a cone of radius $\Delta R = 0.2$ around the direction of lepton emission.

It must be mentioned that standard parametrization in the ATLFAST has been used for the leptonic resolution but detailed studies are needed, using test beam data and GEANT full simulation to validate the extrapolation of the resolution function to leptonic energies in the TeV range.

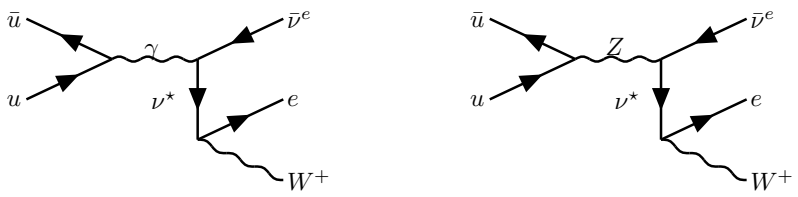

Fig. 4. Production and decay of excited neutrino ($\nu^\star$) to W and electron (e).

3.1 $q\overline{q} \rightarrow \nu^\star\nu$ subprocess

For this type of subprocess, we consider only the decay of excited neutrino to a W and an electron mediated by gauge interactions. Typical Feynman diagrams relevant for this process are shown in Fig. 4.

For the W decay, we limited ourselves to the case $W \rightarrow$ jets. In the case of semileptonic decays of W, the final state consists of two neutrinos, giving a large uncertainty in the excited neutrino mass reconstruction.

The signal signature for the selected reaction ($\nu^\star \rightarrow We$) consists of an electron and two jets. We considered three SM backgrounds:

- $t\bar{t}$ pair production, where one W decays to jets and the second W decays into an electron and a neutrino.
- WW pair production with the same decays as above.
- $W + jets$ production, where W is allowed to decay to an electron and a neutrino.

The following cuts were used to separate the signal from background:

- The electron was required to be emitted in the pseudorapidity region $|\eta| < 2.5$ and its transverse momentum was required to be at least 150 (250, 300) GeV for $m^\star$ masses of 500, (750, 1000) GeV, respectively.
- The transverse momenta of two jets were required to be at least 50 GeV.
- It was required to have W mass reconstructed with two jets in the $60-100$ GeV mass window (mainly to suppress the dominant $W + jets$ background).
- The missing transverse momentum cut, $\not{P}_T$, was required to be at least 300 GeV.

The resulting invariant mass distributions of the (electron-jet-jet) system are presented in Fig. 5 for the mass of the excited neutrino $m^\star = 500$ GeV (left) and $m^\star = 1000$ GeV (right).

The resonances are clearly seen above the total background. The distributions were normalized to an integrated luminosity of $L = 300$ fb^{-1}.

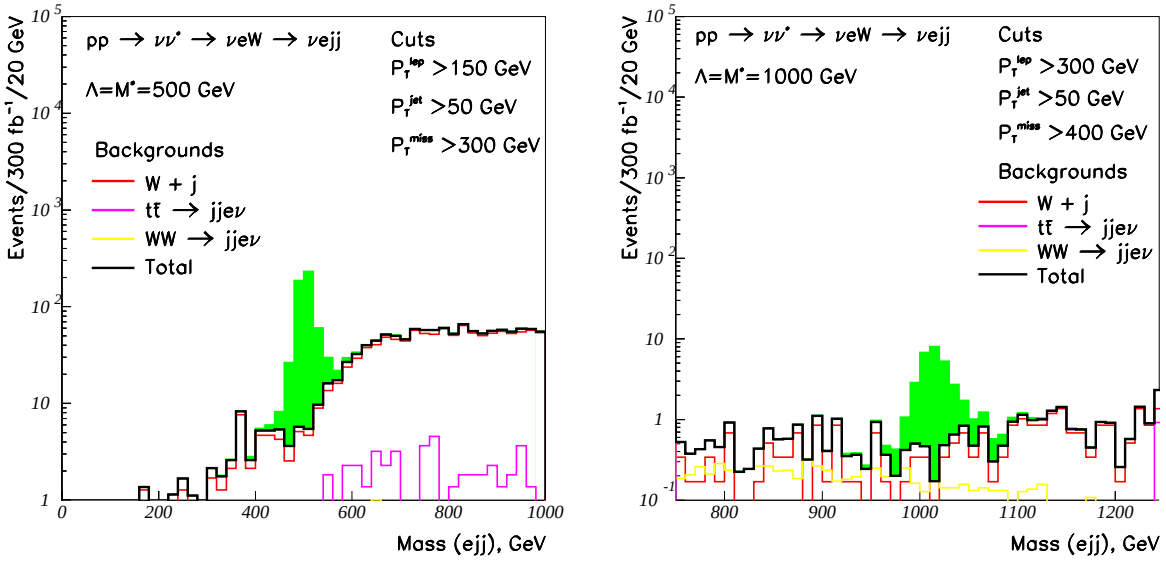

Fig. 5. Invariant mass distributions of $\nu^\star$ ($\rightarrow We$) and W's decay to jets for $m^\star = 500$ GeV (left) and $m^\star = 1000$ GeV (right). The integrated luminosity is $300 fb^{-1}$.

3.2 $q\overline{q} \rightarrow e\nu^\star$ subprocess

3.2.1 $\nu^\star \rightarrow We$ decay channel. Here again we considered the decay of excited neutrino to We mediated by gauge interactions (Fig. 6).

We have studied cases with W decay to jets, as well as, with semileptonic decays of W into an electron and a neutrino.

In the case of W decay to $e\nu$, the final state consists of three electrons and a neutrino. The signal signature is sought in the system of two electrons and a neutrino.

For this final state we studied two SM backgrounds:

- $W + Z$ production where W decays to $e\nu$ and Z decays to electron - positron pair.
- WWW production, where all three W allowed to decay only into an electron and a neutrino.

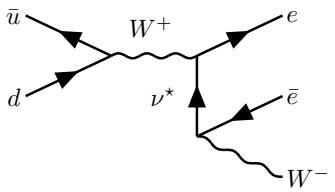

Fig. 6. Production and decay of excited neutrino ($\nu^\star$) to W and electron.

The following cuts were used to separate the signal from background:

- The transverse momenta of three electron were required to be at least 50 GeV, and to be within the pseudorapidity acceptance of $|\eta| < 2.5$.
- It was required to have $W \rightarrow e\nu$ mass reconstructed in the $(70 - 90)$ GeV mass window. This requirement was used as a constraint for obtaining the energy of the neutrino.
- The reconstruction of the two electron masses in the $(80 - 100)$ GeV mass window has been used as a Z production veto to suppress the $W + Z$ background.

In the case of W decays to jets, the final state consists of two electrons and two jets. For this reaction the signal signature consists of an electron and two accompanying jets.

For the relevant SM backgrounds corresponding to this final state we used:

- $Z + jets$ production where Z decays to an electron - positron pair.
- WWW production, where two W's are allowed to decay into an electron and a neutrino and the third W to jets.

For this signal signature, the corresponding cuts used were:

- The transverse momenta of two electrons were required to be at least 150 GeV, and to be within the pseudorapidity region of $|\eta| < 2.5$.
- The transverse momenta of two jets were required to be at least 20 GeV.
- It was required to have the mass of $W \rightarrow$ jets reconstructed in the $(70 - 90)$ GeV mass window, for the suppression of the dominant $Z + jets$ background.
- The reconstruction of the two electron masses in the $(80 - 100)$ GeV mass window also has been used as a veto to suppress the $Z + jets$ background.

The resulting invariant mass distribution is presented in Fig. 7 for the system of two electrons and neutrino (left side) and for the system of electron-jet-jet (right side) for different masses of the excited neutrino. The distributions were normalized to an integrated luminosity of $L = 300$ fb^{-1}.

3.2.2 $\nu^\star \rightarrow Z\nu$ decay channel. The decay of the excited neutrino to $Z\nu$, mediated by gauge interactions, was considered in this section.

The corresponding diagram is presented in Fig. 8.

For the Z decay, we studied the cases where Z decays to jets or Z decays into $\mu^+\mu^-$ pairs.

In the case of Z decays to jets, the final state consists of an electron, a neutrino and two jets. The signal sought for an energetic electron with two accompanying jets in the presence of a large missing transverse energy.

For this signal we considered three SM background:

- $W + jets$ production, where W are allowed to decay into an electron and a neutrino.
- $t\bar{t}$ pair production, where one W decays to jets and the second W into an electron and a neutrino.

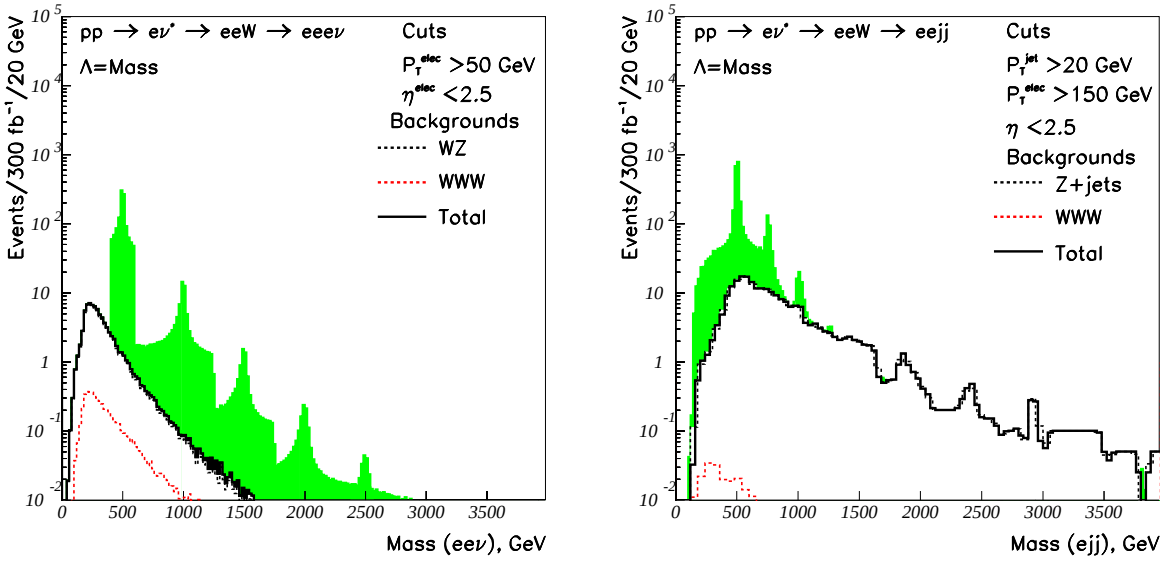

Fig. 7. Invariant mass distributions of $\nu^\star$ ($\rightarrow We$) for the W decay mode to $e\nu$ (left) and to jets (right). The integrated luminosity is $300 fb^{-1}$.

- WW pair production with the same decays as above.

The following cuts were used to separate the signal from backgrounds:

- The transverse momentum of an electron was required to be at least 170 (200, 400) GeV for excited neutrino masses of 500 (750, 1000) GeV and to be emitted within pseudorapidity acceptance of $|\eta| < 2.5$.
- The transverse momenta of two jets were required to be at least 40 GeV.
- It was required to have $Z \rightarrow$ jets mass reconstructed in the $(80 - 100)$ GeV mass window to suppress the dominant $W + jets$ background.
- The missing transverse momentum cut,$\not{P_T}$, was required to be at least 400 GeV.

The resulting invariant mass distributions of the electron-jet-jet system are presented in Fig. 9 for the mass of the excited neutrino $m^\star = 500$ GeV (left). The distribution was normalized to an integrated luminosity of $L = 300$ fb^{-1}.

For the case where Z decays into $\mu^+\mu^-$ pairs, the final state consists of two muons, an electron and a neutrino. The signal signature for this subprocess is two muons and the missing transverse energy, accompanied by an energetic electron.

The natural SM background for this subprocess is the $W + Z$ production where W decays to $e\nu$ and Z decays into muons.

The following cuts were used to separate the signal from the background:

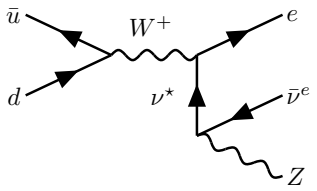

Fig. 8. Production and decay of the excited neutrino ($\nu^\star$) to Z and ν.

- The transverse momentum of an electron was required to be at least 120 GeV within the pseudorapidity of $|\eta| < 2.5$.
- The transverse momenta of two muons were required to be at least 10 GeV.
- The missing transverse momentum cut, $\not{P}_T$, was required to be at least 100 GeV.

The resulting invariant mass distribution of two muons combined with the missing transverse energy is presented in Fig. 9 (right) for an integrated luminosity of $L = 300$ fb^{-1}.

3.2.3 $\nu^\star \rightarrow \nu\gamma$ decay channel. Another interesting subprocess is the decay of an excited neutrino to ν and a photon (Fig. 10).

The signal consists of a photon and a neutrino in the presence of an energetic electron.

The natural SM background for this subprocess is the $W + \gamma$ production where W decays to e and ν.

The cuts used to separate the signal from background are:

- The transverse momenta of an electron and a photon were required to be at least 50 GeV, and to be within the pseudorapidity acceptance of $|\eta| < 2.5$.

The resulting transverse mass distribution of the electron and missing transverse momentum is presented in Fig. 11 (right) for an integrated luminosity of $L = 300$ fb^{-1}.

In Table 3, the corresponding signal significances, obtained for all studied subprocesses, are presented for an integrated luminosity of $L = 300 fb^{-1}$. The number of accepted signal and background events were defined in the selected mass bin width (ΔM). For the mass bin width, the value was taken equal to a $\pm 2\sigma$ width of the invariant mass distribution around the excited neutrino peak's position.

As can be seen from Table 3, the highest reach for excited neutrino production would be available in decays of the excited neutrino to ν and a photon (due to a low background level) for a non-zero $\nu\nu^*\gamma$ coupling at $f = -f' = 1$ but excited neutrino decay channel involving W is also promising. In case of $f = f' = 1$, the $\nu\nu^*\gamma$ coupling vanishes, and excited neutrino decay channel involving W becomes clearly dominant. The mass reach for the decay channel of neutrino with $(eee\nu)$ final state is around 1500 GeV, practically independent from $f = f' = 1$ or $f = -f' = 1$ couplings choice. At lower values of excited neutrino masses the signature with $(eejj)$ in the final state is more promising due to a better statistical significance.

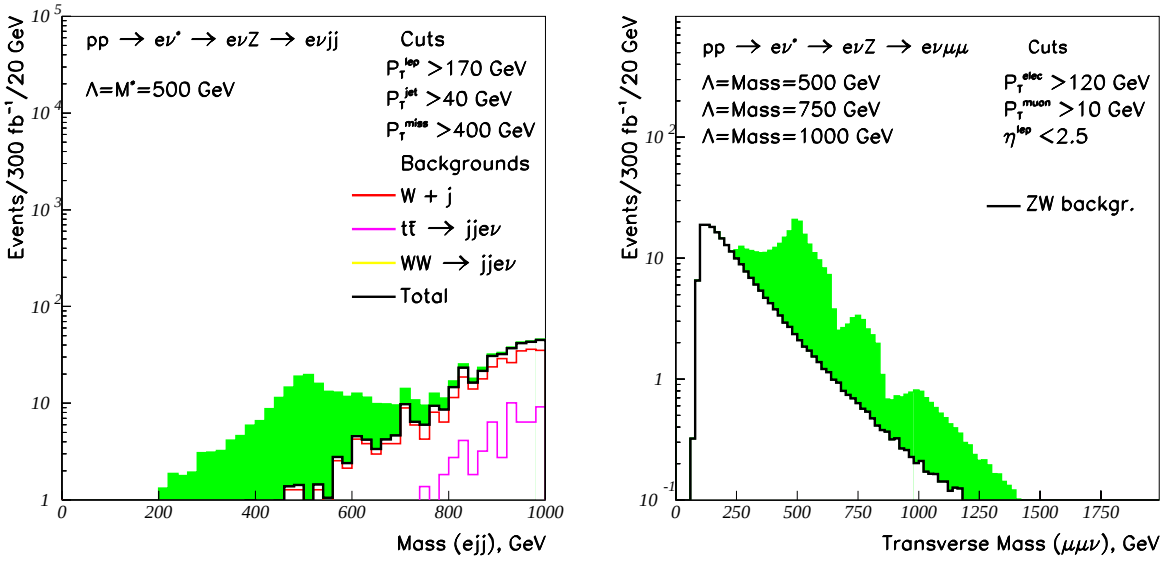

Fig. 9. Invariant mass distributions of $\nu^\star$ ($\rightarrow Ze$) for Z decay mode to jets for $m^\star = 500$ GeV (left) and $\nu^\star$ ($\rightarrow Ze$) for Z decay mode to $\mu^+\mu^-$ (right). The integrated luminosity is $300 fb^{-1}$.

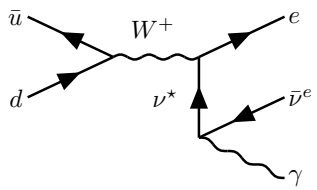

Fig. 10. Production and decay of excited neutrino ($\nu^\star$) to γ and e

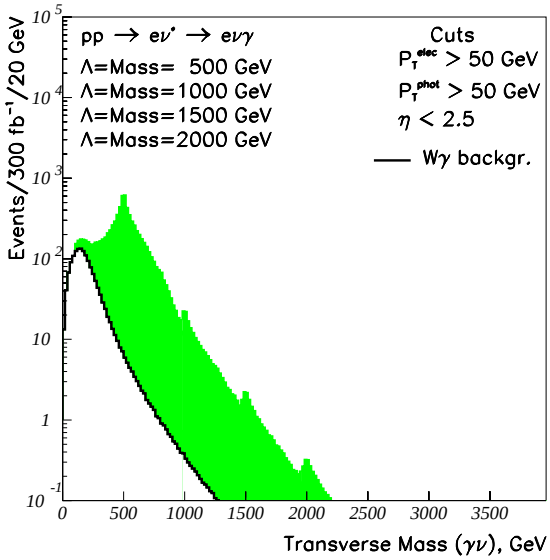

Fig. 11. Transverse mass distribution of $\nu^\star \to \nu\gamma$. The integrated luminosity is $300 fb^{-1}$.

Excited neutrino decay channels involving Z bosons, due to the smaller branching ratio, could be used only to confirm excited neutrino observation, obtained from other channels. This channel could be observable for the $f = f' = 1$ case and m_{ν^*} only below 1 TeV. The case of $f = -f' = 1$ is even less promising and it is not presented in Table 3 — the number of signal events goes down with about factor of 3.5 according to the $\nu^* \to Z\nu$ branching ratio (see Table 2).

4 Conclusions

Based on the prediction of a composite model of quarks and leptons, excited neutrino will be possibly observed at CERN LHC. We have presented the results of excited single neutrinos production and their subsequent decays through gauge interactions. Rather clean signatures are expected to be found for certain decays with neutrino in the final state. We have been studied two cases of f, f' parameters: the case of $f = -f' = 1$ which gives rise to a non-vanishing $\nu\nu^*\gamma$ coupling and the case of $f = f' = 1$. For $f = -f' = 1$, the highest reach is expected for $e\nu\gamma$ final state, while in the case of $f = f' = 1$, $eee\nu$ and $eejj$ final states look most promising to reach large excited neutrino masses. We have found that singly produced excited neutrinos could be accessible up to a mass of 1.5 TeV at LHC, assuming an integrated luminosity of $L = 300 fb^{-1}$.

5 Acknowledgements

This work has been performed within the ATLAS Collaboration with the help of the simulation framework and tools which are the result of the collaboration-wide efforts. We would like also to thank G. Azuelos, H.Baer, O.Çakır, D. Froidevaux, F. Gianotti, I. Hinchliffe, L. Poggioli, L.Reina

Table 3. The signal significances, $S/\sqrt{S+B}$, S for signal, B for total background, and number of events are calculated for an integrated luminosity of $L = 300 fb^{-1}$, $\Lambda = m^\star$ and various couplings within selected mass bin width (ΔM).

$m^\star(GeV) \rightarrow$	500	750	1000	1250	1500
$q\overline{q} \rightarrow \nu\nu^\star \rightarrow \nu eW \rightarrow \nu ejj$, $f = \pm f' = 1$					
ΔM, GeV	28	72	92	116	-
S	472	103	24	5	-
$S/\sqrt{S+B}$	21	10	5	2	-
$q\overline{q} \rightarrow e\nu^\star \rightarrow eeW \rightarrow eee\nu$, $f = \pm f' = 1$					
ΔM, GeV	32	98	100	102	132
S	1097	271	60	26	6
$S/\sqrt{S+B}$	33	16	7	5	2.2
$q\overline{q} \rightarrow e\nu^\star \rightarrow eeW \rightarrow eejj$, $f = \pm f' = 1$					
ΔM, GeV	36	92	120	160	180
S	2015	488	108	23	3
$S/\sqrt{S+B}$	44	20	9	3	1.5
$q\overline{q} \rightarrow e\nu^\star \rightarrow e\nu Z \rightarrow e\nu\mu\mu$, $f = f' = 1$					
ΔM, GeV	100	260	400	-	-
S	123	20	4	-	-
$S/\sqrt{S+B}$	10	4	2	-	-
$q\overline{q} \rightarrow e\nu^\star \rightarrow e\nu Z \rightarrow e\nu jj$, $f = f' = 1$					
ΔM, GeV	160	240	320	-	-
S	141	36	6	-	-
$S/\sqrt{S+B}$	29	5	2	-	-
$q\overline{q} \rightarrow e\nu^\star \rightarrow \gamma e\nu$, $f = -f' = 1$					
ΔM, GeV	120	160	200	204	240
S	4218	546	196	63	27
$S/\sqrt{S+B}$	64	23	14	8	5

for their comments about the subject. C.L. and R.M. thank NSERC/Canada for their support. This research was partially supported by the U.S. Department of Energy under contracts number DE-FG02-97ER41022 and DE-FG03-94ER40833.

References

1. H.Terazawa, M.Yasue, K.Akama, M.Hayashi: Phys.Lett. B **112** (1982) 387
   F.M.Renard: Il Nuovo Cimento, **77**A (1983) 1
   A. De Rujula, L.Maiani, and R.Petronzio: Phys.Lett. B **140** (1984) 253
   E.J.Eichten, K.D.Lane, and M.E.Peskin: Phys.Rev. D **50** (1983) 811
2. H.Terazawa, Y.Chikashige, and K.Akama: Phys.Rev. D **15** (1977) 480
3. Y.Ne'eman: Phys.Lett. B **82** (1979) 69
4. U.Baur, M.Spira, and P.M.Zerwas: Phys. Rev. D **42** (1990) 815
5. P. Achard *et al.* [L3 Collaboration], Phys. Lett. B **568**, 23 (2003) [arXiv:hep-ex/0306016]; S. Andringa *et al.* [DELPHI Collaboration], CERN-OPEN-99-469 *Prepared for 34th Rencontres de Moriond: Electroweak Interactions and Unified Theories, Les Arcs, France, 13-20 Mar 1999*; B. Vachon, Nucl. Phys.

Proc. Suppl. **98**, 148 (2001); R. Barate *et al.* [ALEPH Collaboration], Eur. Phys. J. C **12**, 183 (2000) [arXiv:hep-ex/9904011].
6. L. Bellagamba [H1 and ZEUS Collaborations], *Prepared for 31st International Conference on High Energy Physics (ICHEP 2002), Amsterdam, The Netherlands, 24-31 Jul 2002*; U. F. Katz [H1 Collaboration], arXiv:hep-ex/0212049; C. Adloff *et al.* [H1 Collaboration], Phys. Lett. B **548**, 35 (2002) [arXiv:hep-ex/0207038]; A. Weber, Acta Phys. Polon. B **33**, 3899 (2002) [arXiv:hep-ex/0207032]; C. Adloff *et al.* [H1 Collaboration], Phys. Lett. B **479**, 358 (2000) [arXiv:hep-ex/0003002].
7. E. Boos, A. Vologdin, D. Toback and J. Gaspard, Phys. Rev. D **66**, 013011 (2002) [arXiv:hep-ph/0111034]; J. A. Green [D0 Collaboration], arXiv:hep-ex/0004035; B. Abbott *et al.* [D0 Collaboration], Phys. Rev. Lett. **82**, 4769 (1999) [arXiv:hep-ex/9812010]; A. Bodek [CDF Collaboration], Nucl. Phys. Proc. Suppl. **66**, 96 (1998). E. Gallas [D0 Collaboration], FERMILAB-CONF-97-390-E *To be published in the proceedings of International Europhysics Conference on High-Energy Physics (HEP 97), Jerusalem, Israel, 19-26 Aug 1997*; P. deBarbaro, A. Bodek, B. J. Kim, Q. Fan and R. Harris [CDF Collaboration], FERMILAB-CONF-96-356 *To be published in the proceedings of 1996 DPF / DPB Summer Study on New Directions for High-energy Physics (Snowmass 96), Snowmass, CO, 25 Jun - 12 Jul 1996*
8. U. Baur, I. Hinchliffe and D. Zeppenfeld, Int. J. Mod. Phys. A **2**, 1285 (1987);
9. O. Cakir and R. Mehdiyev, Phys. Rev. D **60**, 034004 (1999); O. Cakir, C. Leroy and R. Mehdiyev, Phys. Rev. D **62**, 114018 (2000); O. Cakir, C. Leroy and R. Mehdiyev, Phys. Rev. D **63**, 094014 (2001).
10. O. J. P. Eboli, S. M. Lietti and P. Mathews, Phys. Rev. D **65**, 075003 (2002) [arXiv:hep-ph/0111001].
11. O. Cakir, C. Leroy, R. Mehdiyev and A. Belyaev, Eur. Phys. J. directC **30**, 005 (2003) [arXiv:hep-ph/0212006].
12. J. H. Kuhn and P. M. Zerwas, Phys.Lett. B 147 (1984) 189;
    J. H. Kuhn, H. D. Thoel and P. M. Zerwas, Phys. Lett. B 158 (1985) 270.
13. F. M. Renard, Phys. Lett. B 116 (1982) 264
14. N. Cabibbo, L. Maiani and Y. Strivastava, Phys. Lett. B 139 (1984) 459;
    F.M Renard, Phys. Lett. B 126 (1983) 59, B 139 (1984) 449;
    K. Hagiwara, S. Komamiya and D. Zeppenfeld, Z. Phys. C 29 (1988) 265.
15. , "ATLAS detector and physics performance. Technical design report. Vol. 2," CERN-LHCC-99-15
16. R.Barate et al.: Eur.Phys.Jour. C **12** (2000) 183
17. B.Abbott et al.: Phys.Rev.Lett. **82** (1999) 4769
18. J.Breitweg et al.: Z.Phys. C **76** (1997) 631
19. G.Abbiendi et al.: Phys.Lett. B **465** (1999) 303
20. H.L.Lai et al., CTEQ Coll.: Eur.Phys.J C **12** (2000) 375
21. M.Glúck,E.Reya and A.Vogt: Z.Phys C **53** (1992) 651
22. H.L.Lai et al., CTEQ Coll.: Phys.Rev. D **51** (1995) 4763
23. T.Sjostrand: Computer Phys. Communications **82** (1994) 74
24. A.Pukhov at al., hep-ph/9908288 (1999)
25. A. S. Belyaev *et al.*, hep-ph/0101232.
26. E.Richter-Was, D.Froidevaux and L.Poggioli: ATLAS Note PHYS-98-131 (1998)
27. Technical Proposal, ATLAS Coll.: Report No. CERN/LHCC/94-43
28. ATLAS Detector and Physics Performance Technical Design Report
    CERN/LHCC/99-14, (1999)